Land-cover Change and Vulnerability to Flooding near Poyang Lake, Jiangxi Province, China

Luguang Jiang, Kathleen M. Bergen, Daniel G. Brown, Tingting Zhao, Qing Tian, and Shuhua Qi

Abstract

Inhabitants near Poyang Lake, in the Central Yangtze River Basin, China, are vulnerable to loss of life and livelihood because of the interactions of flooding and land-use policies and decisions. We analyzed implications of land-cover patterns for vulnerability to flooding in the Poyang Lake Region. Land-cover and change were mapped using multi-temporal Landsat TM/ETM+ images at high and low water levels from 1987, 1993, 1999, and 2004. Vulnerability to flooding was analyzed based on the distribution of land covers relative to elevation and the levee quality. Results showed that patterns of Farmland, Urban, and Wetland covers varied by elevation, by the relative likelihood of flooding within polders, and over time; the general trend, with some notable exceptions, was toward less vulnerability of farmland and urban areas to flooding. Factors of markets, laws and regulations have likely influenced changes in land-cover patterns and, therefore, in vulnerability.

Introduction

To support China's population, which grew from 540 million in 1949 to 1.3 billion in 2006, agricultural self-sufficiency, especially in grain production, has been one of the central goals of the Chinese government. Because of a limited area of farmland per capita and inefficient farming methods, historically the primary means of increasing the total amount of agricultural yield has been to enlarge the farmland area. One consequence of this has been the conversion of large areas of natural wetlands in fertile areas, such as those in the Central Yangtze Basin, to farmland (wetland reclamation). During the past twentieth century, many levees were built to encircle new farmland in low elevation areas adjacent to lakes and rivers, forming polders that are protected against flooding (Zhao *et al.*, 2003). In 1984, the Chinese government declared that agricultural grain self-sufficiency had been reached and certain land-use policies were reconsidered (Rozelle *et al.*, 1997). Beginning in 1986, wetland reclamation was banned, and laws have promoted restoring some reclaimed farmland back to natural wetland (wetland restoration).

In addition to the policies and laws regulating the conversion of wetlands and farmlands, grain markets have also had an impact on land-use. Beginning in the early 1990's, China has transitioned from a planned economy, where grain prices were fixed by the government, to a market economy, where prices have been determined mainly by the grain market. Grain prices increased gradually in the period from 1980 to 1993, very rapidly from 1993 to 1997, and then decreased between 1997 and 2003 (Statistics Bureau of Jiangxi Province, 2004). In response to the recent decrease, the central government exempted farmers from agricultural taxes in 2004 to encourage farmers' activity in grain production (Gale, 2005). In the transitioning economy, the trend has also been toward greater and more rapid economic growth and urbanization, including rural farming and wetland areas. Over time, intense land-use and human settlement in the floodplains of the Central Yangtze Basin have exposed millions of people to flooding hazards in that region. We used the distribution and changes of natural (e.g., wetlands and water) and human-managed land covers (e.g., urban and agriculture) over an approximate 20-year period to evaluate the vulnerability of a population and how it has changed as a result of these recent policy and economic changes.

The Poyang Lake Region (PLR) in the Central Yangtze River Basin in Jiangxi Province is an important regional example of such interactions between government policies, human land-use, and natural flooding regimes. The goal of this study was to determine the changes in PLR land covers over time, especially between farmland, wetland, and urban, and then to analyze and interpret them across elevation zones and polder types to assess changes in the vulnerability of the population to flooding. The specific objectives were to: (a) compile spatial data, including digital elevation models (DEMs), polder maps, land-cover maps and land-cover-change probabilities between 1987 and 2004, both of the last two being derived from multi-temporal Landsat

Luguang Jiang is with the Institute of Geographical Sciences and Natural Resources Research, Chinese Academy of Sciences, Beijing, China.

Kathleen M. Bergen, Daniel G. Brown and Qing Tian are with the School of Natural Resources and Environment, University of Michigan, 440 Church St., Ann Arbor, MI 48109 (danbrown@umich.edu).

Tingting Zhao is with the Department of Geography, Florida State University, Tallahassee, FL.

Shuhua Qi is with the Key Lab of Poyang Lake Ecological Environment and Resource Development, Jiangxi Normal University, Nanchang, Jiangxi, China.

Photogrammetric Engineering & Remote Sensing
Vol. 74, No. 6, June 2008, pp. 775–786.

0099-1112/08/7406–0775/$3.00/0
© 2008 American Society for Photogrammetry and Remote Sensing

Thematic Mapper (TM) and Enhanced Thematic Mapper+ (ETM+) data; (b) assess patterns and changes in land-cover based on elevation and the quality of polders; and (c) interpret the spatial distribution of the land system in terms of flood vulnerability in the PLR. The results contribute to a conceptual model of the complex relationships between policy, human activities, land-cover change and flood vulnerability.

Background

Land-based Vulnerability Assessment

Vulnerability to natural hazards is affected by a combination of variability in the (a) natural processes that expose human communities to harm, and (b) variability in the ability of those communities to respond or adapt to those natural processes. While a general understanding of hazards as they result from both human and natural dynamics has been in place for decades (e.g., White and Haas, 1975), a truly integrated understanding has only recently become attainable, partially through new observational and analytical tools that provide better opportunities for rigorous spatial and temporal studies of coupled human-environment systems (Liverman *et al.*, 1998). Although remote sensing has been applied to flood dynamics and damage assessment (Xiao *et al.*, 2002; Wang *et al.*, 2003), there has been less work relating these contemporary methods and tools with broad vulnerability frameworks to study the effects of flooding on human vulnerability (Ojima *et al.*, 2004). There is an opportunity to use remote sensing to assess the interaction between flood risk and human activity, as indicated by human-managed land covers.

Land Policy and the PLR

The PLR lies within the Central Yangtze River Basin which is one of the most important and fertile grain production areas of China. During the twentieth century, Poyang Lake, and other lakes of the Central Yangtze Basin, lost large areas of wetlands due to their reclamation for farmland, and the natural capacity of the lakes and wetlands for flood regulation shrank significantly. The flood frequency in the region increased and the Central Yangtze Basin, including the PLR, suffered disastrous floods, especially in 1995, 1998, and 1999 (Min, 2004; Shankman and Liang, 2003; Yin and Li, 2001). After the largest flood disaster of 1998, a wetland restoration policy called "returning farmland to lake" was launched by the central government and applied to four provinces within the Central Yangtze Basin, with a particular focus within the PLR. According to the policy, a number of polders that had been reclaimed for agriculture were to be returned to natural lake and wetland areas by destroying the levees that maintained them. While these new policies have shifted towards restoration of some wetlands near Poyang Lake, the PLR is still one of the most important grain production regions in China.

Land Cover in the PLR

Based on annual government statistical data on farmland area from 1949 to 2002, Liu (2005) showed that farmland area in PLR increased continuously from 1949 to 1957, but decreased continuously from 1957 to 2002. While remote sensing data are not available for such long-term analysis, they have the advantage of being objective and spatially explicit representations of the landscape. With its 30+ years of operation, the Landsat platform has become an extremely useful tool in mapping long-term land-cover trends and relating these trends to broader environmental, societal, and policy shifts. Land-cover is a useful indicator of human activity, especially in the predominantly agricultural landscape of the PLR (Zhao and Fang, 2004). Land-cover patterns indicate where human lives and livelihoods are tied to specific locations, e.g., where residences are located and where crops are grown. An important advantage of using land-cover as an indicator of human activity for vulnerability assessment is that the spatial distributions of activities can be mapped at relatively fine spatial resolutions and over time.

In the mid-1980s, a remote sensing survey of land-cover was conducted by the Chinese Academy of Sciences (CAS) and the government of Jiangxi Province. This study reported that farmland in the PLR in 1985 was 57 percent larger than that reported in official statistics for the same date (Editorial Committee of Poyang Lake Research, 1988). Rao *et al.* (2002) investigated land-cover change between 1988 and 1998 in the PLR using 30-meter Landsat TM images. Results indicated that the area of farmland in the PLR decreased from 7,949 km^2 in 1988 to 7,054 km^2 in 1998, while the area of wetland increased from 4,148 km^2 to 4,701 km^2 in the same period. The area of farmland derived from this analysis was also about 58 percent higher than the figures in the government annual statistical data. While it is possible that actual farmland may be more comprehensively counted using remote sensing methods than statistical censuses, it is also possible that it may have been overestimated in the remote-sensing-based studies because of spectral confusion of the farmland with natural grassland (Li and Liu, 2001; Rao *et al.*, 2002).

The analysis by Rao *et al.* (2002) also suggested two additional important patterns relevant to flooding and vulnerability. First, between 1988 and 1998 there was a 53 percent increase in the built-up area of the PLR (to approximately 2 percent of area in 1998), tracking a 13 percent increase in population from 1988 to 1998 and rapid economic growth. Second, an analysis of cover types by landform (i.e., coastal zone, uplands, hills, and mountains) revealed that about 80 percent of the built-up area and 60 percent of the farmland occurred in the coastal zone (<30 m elevation) class, which made up 50 percent of the region. By contrast, only about 5 percent and 20 percent of the forest and grassland/shrubland land covers occurred in the coastal zone class, respectively. Based on this work, it can be inferred that within the PLR, human activity is disproportionately represented within the area most affected by flood dynamics.

Study Site

The Poyang Lake watershed is approximately 162,225 km^2 and encompasses nearly all of Jiangxi Province. The Poyang Lake Region (PLR) is defined in this study as the 12 counties (19,904 km^2) around Poyang Lake and within Jiangxi Province that contain portions of Poyang Lake itself (Figure 1). The study site analyzed for this study encompasses nearly all of the PLR, consisting of the portion of the PLR (approximately 88 percent; 16,953 km^2) present within the footprint of Landsat WRS-2 path 121/row 40. This Landsat path/row and study site is centered on 116° 24′ E and 28° 53′ N. The climate in the site is subtropical, warm, and wet with an average annual temperature of approximately 17°C and average annual precipitation of 140 to 190 cm. The subtropical monsoon climate has two distinct seasons, a wet season, generally April to September, and a dry season, generally October to March.

The largest and most dynamic feature in the study site is Poyang Lake, the largest freshwater lake in China (Figure 1). The lake lies in a shallow structural depression and stretches 170 km north-south, 74 km east-west with a coastline of about 1,800 km in high-water season. It has a surface area of approximately 3,850 km^2 in the high-water season, but no more than 1,000 km^2 in low-water seasons. The lake water is

Figure 1. Study site and surrounding area. Shown on the lower map is the location of the PLR China. Shown on the upper map is the PLR (twelve counties) and the study site (portion of the twelve counties within Landsat TM/ETM+ path 121/row 40) overlaid on the Landsat TM 2004 high water image.

fed mainly by the Ganjiang River system, but also the Fuhe, Xinjiang, Raohe, and Xiushui, and drains north into the Yangtze River. Due to monsoon climate annual wet and dry cycles, consequent fluctuations in the Yangtze River levels, and a shallow bathymetry, Poyang Lake experiences large seasonal fluctuations in water levels with a range of 12 m between low to high water levels on average (use of "m" here and subsequently refers to meters above mean sea level, according to the 1985 National Vertical Datum of China; NVDC 1985). According to water-level records from the Hukou hydrological station, near the lake's outlet, the maximum water level was 20.7 m in 1998, and the minimum water level was 4.1 m in 1963. The high water results from a combination of greater south to north river inflow from the Ganjiang and other watersheds and the reverse flow of Yangtze floodwaters from north to south into the lake basin (Shankman and Liang, 2003). This combination causes the lake to spread in its basin rather than draining out through the Yangtze. In 1998, there were about 6,400 km of levees in the PLR, which serve to partially restrain the lake extent during the flood season.

The total population of the PLR is 8.86 million people, 68 percent of which are rural, i.e., they have permanent residences registered in what are officially considered rural areas consisting of farmland (Statistic Bureau of Jiangxi Province, 2004). Cities, including Nanchang (population 1.9 million) and Jiujiang (population 0.6 million), form major regional centers. Most rural households participate in agricultural production or associated commerce. Fishing is also an important local source of income. The lake and its wetlands also provide habitat for over a half million migratory waterbirds of at least 150 species, including internationally important and threatened species. Rao *et al.* (2002) provide an approximation of the land-cover status of the study site at the beginning of the study period. In 1988, the dominant land-cover in the PLR was farmland, about 40 percent of land area. This was followed in size by shrub-grassland cover on steeper slopes (21 percent), forests (14 percent), and urban (1.8 percent). The remainder of the area was characterized as consisting of permanent water and seasonal water/wetlands areas.

Data and Methods

Landsat TM/ETM+ Data

Four pairs of Landsat TM/ETM+ imagery for path121/row40 were acquired for the purpose of mapping major land-cover types across the study area in 1987, 1993, 1999, and 2004 (Table 1). Each image pair consisted of a winter scene acquired between December and February, and a summer scene from July. Six of the eight images were orthorectified using a DEM developed from contours mapped at a scale of 1:50 000 (described below); the two remaining scenes had been orthorectified by Earth Satellite Corporation (EarthSat) based on their global geodetic control points (Tucker *et al.*, 2004). Each pair of images was geometrically registered, and then the pairs (including the EarthSat images) were registered to each other using the 2004 pair as the base. The total RMSE for registration of all images was less than 15 m. This resulted in a matched set of images in the WGS84 datum and UTM projection. Areas covered by clouds or cloud shadows in any image were removed from all images.

The Landsat TM/ETM+ bands, except thermal, were processed to at-sensor reflectance to remove effects of different solar incident angles (Irish, 1998; Chander and Markham, 2003). Eighteen spectral features were derived as candidate classification features. These included the first six principal components of the bi-seasonal at-sensor reflectance, six Tasseled Cap indices (three from each season), two normalized difference vegetation indices (NDVI), two normalized difference water indices (NDWI), and two rice indices (ratio of the summertime band5/band4 and band3/band2: Shibayama, 1989; Li, 2001). After removing correlated spectral features,

Table 1. Landsat TM/ETM+ Data Used in Land-cover Classification. China RSGS Refers to the China Remote-Sensing Satellite Ground Station of the Chinese Academy of Sciences, and EarthSat to Earth Satellite Corporation

Image Pair	Imaging Date	Sensor	Source
1	17 December 1987	Landsat-5 TM	China RSGS
	15 July 1989	Landsat-5 TM	EarthSat
2	31 January 1993	Landsat-5 TM	China RSGS
	10 July 1993	Landsat-5 TM	China RSGS
3	10 December 1999	Landsat-7 ETM+	EarthSat
	05 July 2000	Landsat-7 ETM+	China RSGS
4	15 February 2004	Landsat-5 TM	China RSGS
	24 July 2004	Landsat-5 TM	China RSGS

eight features used in the land-cover classification process and consisted of the six principal components, wintertime Tasseled Cap greenness, and summertime ratio of band3/band2.

Reference Data

Field reference data were collected for 131 locations, randomly chosen from areas that were relatively easy to access with vehicles and by foot. While it would have been preferable to have additional reference points, given the number of classes, the cost of travel to the study area limited our ability to collect more. Nonetheless, we believe the number of sample points is sufficient to indicate the relative level of accuracy of the data and where confusions may exist among classes. Data were collected in January and July 2006 and included all target land-cover classes. Because these data were collected in 2006 and the Landsat TM/ETM+ data were taken prior to that time (1987 to 2004), changes of land-cover had occurred at some of the reference locations. We discarded two of the reference points because they had clearly changed in the previous year (i.e., between 2004 and 2006). Additionally, prior to use of the Landsat TM/ETM+ imagery for classification we compared the 2006 reference data class label with the 1987, 1993, and 1999 image composites and available ancillary data and modified reference data class labels for any sample points that had obviously experienced change. Ancillary data used for this purpose and in the classification process included photos taken at each field reference data point, other remote sensing-derived classifications from a similar set of years (Data Center for Resources and Environmental Sciences, Chinese Academy of Sciences, 2003) and topographic maps (State Bureau of Surveying and Mapping of China, 1972). The reference data compilation resulted in four reference data layers, each applicable to one of the four image years, which were used to aid in Landsat feature selection and to conduct accuracy assessment.

DEM Data

A digital elevation model (DEM) of the PLR, at a resolution of 25 meters, was interpolated from 1:50 000 topographic maps by Jiangxi Provincial Bureau of Surveying and Mapping. The source data had a 5 m contour interval in lowland/plains areas and 10 m contours in hilly areas, and were supplemented in interpolation by additional elevation control points. In addition to use for image orthorectification, the DEM was used to analyze the vertical distributions of land-cover and change. The lowest elevation in the DEM is 12 m, the surface height of Poyang Lake when the topographic map was created. The range of elevations in the study site is 12 m to 1,474 m, with 95 percent of the elevation range falling below 100 m (the remainder being a localized occurrence of a rock-dominated mountain that rises abruptly from the plain). In order to determine the vertical distributions of land-cover and change, and to analyze vulnerability to flooding based on these distributions, the DEM was used to (a) restrict the subsequent area of analysis to elevations less than 100 m, and (b) to divide the study area within the elevation range 12 m to 100 m into 89 one-meter elevation zones.

Levee and Polder Data

The levee and polder system in the PLR protects large areas of land from floods and is comprised of different types of construction erected over a number of years. While the use of levees dates back several centuries, the tremendous flood of 1954 shortly after the foundation of the People's Republic of China, nearly destroyed all of the levees in PLR. After that, the former levees were rebuilt and reinforced between the 1950s and 1970s and some new levees were built to enlarge the farmland area. After 1984, the government no longer encouraged building new levees and polders. After the 1998 flood, levees of important polders were reinforced and some small polders were designated to be restored back to wetland.

Levee locations and types were interpreted and mapped from Landsat TM April 1998 imagery (Jiang, 2006), published data (Jiangxi Province Department of Water Resources, 1999) and field reconnaissance. Levees formed either closed polygons, i.e., human-built levees completely surrounded a polder, or were linear features that connected two points on a coastline, with the remainder of the polder formed by coastlines with elevations above high-water level. The areas of the latter polders were calculated by using the Hydrological Analysis Module of ArcGIS® (ESRI, 2007). The area inundated by the maximum flood (with a lake level of 20.75 m) if there were no levee, was mapped as the protected area for this kind of polder. The polders created by levee mapping were classified into six types differentiated according to their importance, which in turn was determined by how much farmland the polder contains and whether the polder contained small or large urban areas. (Table 2 and Figure 2; Jiangxi Province Department of Water Resources, 1999).

TABLE 2. LEVEE AND POLDER TYPES AND CHARACTERISTICS

Levee Characteristics		Polder Characteristics		
Type	Construction	Amount of Protected Farmland	Urban Area	Flood Risk
Most Important	Concrete, high	>66.7 km^2	Contain large cities	Low
Important	Concrete, high	33.33 to 66.67 km^2	Contain large towns	Low
Small	Concrete, low or Earthen	<33.33 km^2	Do not contain cities or large towns	Moderate
Storage	Concrete	May contain farmland	Little urban area	Low, except high during extreme floods
Partial Return	Earthen	May contain minimal farmland	None (resettled)	High (flood frequency of five years [for polders < 6.67km^2] to ten years [for polders > 6.67km^2])
Complete Return	Earthen	None	None (resettled)	Highest (flood frequency two per three years)

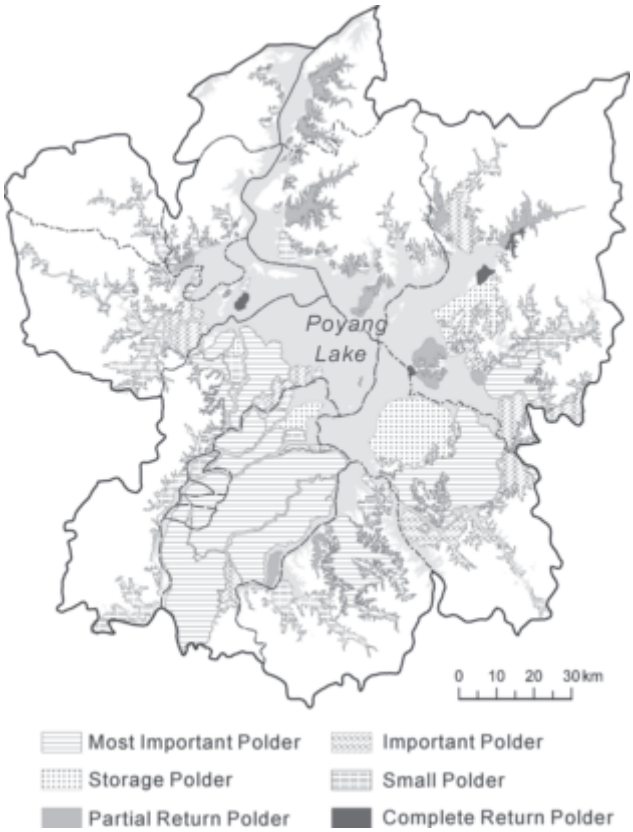

Figure 2. Polders created by different types of levees in the twelve-county PLR.

In the PLR a total area of 5,082 km^2 is in polders and this equals about 57 percent of the flood prone area of the PLR (defined as the area below 20.75 m), with the remainder being mainly the permanent and seasonal water area of the lake (Jiang, 2006).

Precipitation and Temperature Data

Because land-cover of the PLR is strongly linked to dynamic moisture conditions, remote-sensing-based land-cover classifications can be influenced by weather conditions. Therefore, daily data on precipitation and temperature were collected for the study site at and prior to the image dates (China Meteorological Administration, 2007). Daily temperature and precipitation were plotted for each of the four years for the 30 days prior to and including the Landsat TM/ETM+ image date. These data were used to assess anomalous precipitation and temperature patterns as they might affect image classification procedures and interpretations of the classification results.

Land-cover Classification

The ISODATA unsupervised classification algorithm (Tou and Gonzalez, 1974) in Imagine® (Leica Geosystems, 2005) was used to produce eighty clusters of spectrally similar pixels, labeled based on ancillary data. Initially, these spectral clusters were labeled to seven general land-cover categories: Paddy Rice, Upland Crops, Forest, Wetland/Water, Fishpond, Urban, and Bare land. However, when evaluated against ancillary and reference data, early classifications showed that the greatest confusion was between Paddy Rice and Upland Crops (often vegetables or orchards), and therefore these were combined into a single Farmland category in the final classification. The Forest/Shrublands class includes forest plus natural shrublands and mixed shrub/grassland. The Wetland/Water class includes all areas of water, whether permanent water or seasonally inundated lake water and wetlands. Some areas of seasonally inundated grasslands on the lake side of polders were initially classed as Crop (i.e., paddy rice), and these were re-classed as Wetland/Water using knowledge-based methods using the polder map. A similar method was applied within polders (with exception of Partial and Complete Return polders) where flooded areas can be consistently interpreted as rice paddy. Urban includes all built-up areas, whether cities, towns, or rural villages. There are a number of fishponds (inland fish farms) in the study area, and these were mapped separately from Wetlands/Water. The Bare category is comprised of some sand dunes around Poyang Lake but may include any other bare land at the time of image acquisitions (such as lands transitioning to development) (Table 3). Spectral data alone were insufficient to identify fishponds, so this class was identified using spectral, texture and shape characteristics through the object-oriented classifier provided in the Definiens® Professional 5.0 software (Definiens, 2006).

The accuracies of land-cover classifications were examined using the reference data described above. Standard error matrixes were generated (Congalton and Green, 1999) for each date. The producer's and user's accuracy were calculated for each land-cover class, and the overall accuracy and kappa statistic were calculated for all classes combined.

After accuracy assessment, the proportions of each land-cover class for each of the four dates were extracted. The land-cover data were then combined with the DEM, and land-cover proportions for each image date for all land-cover

Table 3. Definitions of the Land-cover Categories and the Combinations of Spectral Classes Used to Create Them

Code	Class Name	Spectral Class Combinations	Description
1	Farmland	Paddy Rice	Rice grown in paddies
		Upland Crops	Upland vegetable and small bush crops/orchards
2	Forest/Shrublands	Forest/Shrublands	Forests (natural and planted)/natural shrub/grasslands
3	Water/Wetland	Water	Permanent water
		Wetland	Seasonally inundated areas
4	Urban	Urban	City/town/village
5	Fishpond	Fishpond	Ponds created specifically for aquaculture
6	Bare	Bare	Bare ground

classes were calculated for each 1 m elevation zone. The land-cover results for the low elevation area below 21 m were then further segmented by polder type and land-cover proportions similarly calculated.

Land-cover Change Probabilities

The next step was to calculate land-cover change for three time periods: 1987 to 1993, 1993 to 1999, and 1999 to 2004. Given slight positional uncertainties and inaccuracies in the pixel-based classification in the images, a probabilistic approach to calculating the land-cover change for each pixel was adopted. First, the probability of each class occurring at a given pixel on a given date was determined using a 3×3 moving window on the classified map and calculating the proportion of the nine pixels in the window that belonged to each class. The 3×3 window size was used to account for possible misregistration among images, which given the 15 m RMSE achieved during orthorectification, we expected would not to exceed one pixel. For each year, six probability layers were then created, one for each class, for a total of 24 layers across the four times. Next, the probabilities of specific land-cover changes were calculated by multiplying probabilities for two classes from two different dates (e.g., between farmland in 1999 and wetland in 2004). Because there were six land-cover classes, there were a total of 36 layers of land-cover-change probabilities for each change period, and a total of 108 change probabilities for the three periods. The resulting maps reflect the probability that each cell transitions from one type to another, depending on how many cells of each of the types are in the neighborhood surround the cell.

Land-cover-change probability was then analyzed by elevation to understand the vertical distribution of land-cover and change. The land-cover change probability data were overlaid on the DEM, and the following were calculated for each elevation zone: (a) the average probabilities of land-cover changes for each change period for all land-cover classes, and (b) the transitions between the key land-cover types of Farmland, Urban, and Wetland for each change period.

Interpretation of Vulnerability

The results of the above land-cover and land-cover-change analysis were interpreted to describe how land-cover and changes are distributed relative to elevation and polder type and how those distributions and changes affect the vulnerability of the populations to flooding. These vulnerabilities are further discussed with respect to relationships between policy and land-use in the PLR.

Results

Classification Accuracies

The land-cover classifications for the four dates had overall accuracies ranging from 81 percent to 86 percent and kappa statistic values ranging from 0.75 to 0.82 (Table 4). Over the four dates, the average producer's accuracy for Farmland (including upland bush crops and orchard) was 80.8 percent. Where farmland was in error, pixels were most often confused with Forest (results not shown). Wetland was classified with an average producer's accuracy of 93.5 percent and was sometimes confused with Farmland (e.g., flooded rice fields). Urban had an average producer's accuracy of 82.9 percent and was most often confused with Bare. Assuming independence of errors in sequential land-cover maps, the estimated overall accuracies of subsequently calculated data on land-cover change for the three change periods, calculated by multiplying overall accuracies for each pair of dates, would be 70 percent (1987 to 1993), 74 percent (1993 to 1999), and 72 percent (1999 to 2004).

Land-cover

Within the PLR, Farmland was the main land-cover type, occupying 41 to 45 percent of the total area in all years; Forest and Wetland/Water together dominated the remaining area at 15 to 21 percent and 29 to 30 percent, respectively, over all years (Table 5). The combined total area of Urban, Fishpond, and Bare was 7 to 10 percent. Among these six land-cover types, Urban and Fishpond are the only two types for which there was a consistent increase in proportion from 1988 to 2004. The greatest rate of increase of Urban occurred between 1999 and 2004. Other patterns varied by date. From 1987 to 1993 and again from 1999 to 2004, the proportion of Farmland increased while the proportion of Forest decreased. Wetland/Water showed a slight increase between 1987 and 1993, but aside from this fluctuation changed little in total proportion over the entire time period of the study.

Weather data analysis showed that conditions antecedent to the dates of image acquisition likely had some impact on the classification results. Bare land occupied a larger area in 1987/1989, and Farmland a smaller area, compared with the other dates. According to the daily records of the Nanchang weather station, there was no effective precipitation 10 days before the 1989 summer image date (05 July 1989 to 15 July 1989), and the temperature was very high (daily maximum temperatures at ~35°C). Areas of sparser dried vegetation may have been spectrally interpreted as Bare. The 1993 summer image occurred shortly after a nine-day period of continuous rain (08 June 1993 to 30 June 1993) totaling 404 mm of precipitation. This caused confusion, especially on land within polders, where rice (Farmland) was spectrally confused with Wetland/Water at that date, although in this case, the polder map was used to distinguish Farmland from Wetland. Also in 1993, Urban was likely underestimated because villages in rural areas were inundated by rainwater. In 1999, when weather patterns were not extreme, the area proportion of Bare land decreased compared to 1987/1989. The year 2004 was a dry year (total precipitation from August 2003 to July 2004 was only 1,027 mm, whereas the average yearly precipitation is 1,624 mm), and the proportion

TABLE 4. RESULTS OF LAND-COVER ACCURACY ASSESSMENT. FOR EACH CLASS, COLUMNS INCLUDE NUMBER OF REFERENCE POINTS AND PRODUCER'S/USER'S ACCURACIES. ALSO GIVEN ARE OVERALL ACCURACY AND THE KAPPA STATISTIC

	Farmland		Forest		Wetland		Urban		Fishpond		Bare		Overall Accuracy	Kappa
	N	P/U%	N	P/U%	N	P/U%	N	P/U%	N	P/U%	N	P/U%	%	
1987	*55*	*71/91*	*32*	*91/85*	*16*	*94/75*	*13*	*85/92*	*9*	*78/100*	*4*	*100/31*	**81.4**	**0.75**
1993	*55*	*87/87*	*31*	*84/87*	*16*	*87/87*	*14*	*79/100*	*9*	*89/100*	*4*	*100/44*	**86.1**	**0.81**
1999	*56*	*82/94*	*24*	*88/78*	*15*	*100/88*	*15*	*87/76*	*12*	*75/100*	*7*	*100/70*	**86.1**	**0.82**
2004	*59*	*83/96*	*22*	*91/91*	*14*	*93/68*	*16*	*81/62*	*10*	*90/100*	*8*	*62/71*	**84.5**	**0.79**

TABLE 5. PROPORTION OF LAND-COVER CATEGORIES IN THE PLR (IN %)

Year	Farmland	Forest	Wetland	Urban	Fishpond	Bare	Total
1987	41.11	21.03	29.23	2.33	0.21	6.08	100.0
1993	45.90	18.06	30.11	2.69	0.35	2.89	100.0
1999	45.88	18.85	28.85	3.80	0.44	2.18	100.0
2004	45.16	15.00	29.01	7.08	0.48	3.27	100.0

of Bare land increased again. Unlike other dates, in 2004, which was a significant fire year, the proportion of Bare land at higher elevation also increased because the burned forest patches were classified as Bare land.

Vertical Distribution of Land-cover

Based on the DEM, the amount of the study area at or below 100 m is 16,138 km^2, or about 95 percent of the study area. The areal proportions of different types of land covers by elevation showed distinct patterns (Figure 3). Over the three time periods, Urban was found at all elevations, with peak prevalence between 18 to 23 m. Farmland had peak abundance between 17 to 30 m. Wetland peaked below 15 m. Overall, above 21 m, the areal proportions of Farmland, Urban area, Wetland/Water and Bare (not shown) decreased with increasing elevation, in contrast to a consistent increase in Forest (not shown). In the elevation zones exposed to possible flooding (i.e., below 21 m), the key land-cover types with respect to vulnerability analysis are Farmland, Urban and Wetland/Water, and these accounted for more than 85 percent of that area in all of the periods. Below 21 m, there was a gradient from Wetland/Water dominance at the lowest elevations to Farmland dominance with increasing elevation.

Vertical Distribution of Land-cover Change 1987 to 2004

In the period 1987 to 1993, the probability of change from Wetland/Water to Farmland below 22 m was much less significant than the reverse change (Figure 4). The trend is in the opposite direction at elevations above 22 m, where the larger transition was from Wetland to Farmland. This relationship was not retained in the period 1993 to 1999, where the change probability from Wetland/Water to Farmland always surpassed the opposite change probability below about 40 m, especially below 30 m. This resulted in a net reduction of Wetland/Water at low elevations between 1993 and 1999. In the period 1999 to 2004, the probability of change from Wetland/Water to Farmland was larger than that from Farmland to Wetland below 17 m. From 17 m to about 60 m, the transition from Farmland to Wetland was the dominant transition. The interchange between the two was relatively balanced at elevations above 60 m.

The intensity of transition from Farmland to Urban land was much higher than that of the transition from Urban area to Farmland in all three periods (Figure 5). The transition probabilities from Farmland to Urban increased over time both in magnitude and over increasingly broader ranges of elevation. The probabilities were greatest in the most recent period, 1999 to 2004. Elevations of peak probabilities of transition from Farmland to Urban were in the range of 19 to 23 m for each period.

Similar to the patterns of transition between Farmland and Urban, the transition probability from Wetland/Water to Urban land was much higher than its reverse transition in all of the three periods (Figure 6). This indicates that in the process of urbanization, some new urban areas were built on the former Wetland/Water areas. Yet, the transition probability values were all very low overall, much lower than those between Farmland and Urban area. Wetlands transitioned to Urban not only at elevations higher than 21 m, but also in the flood risk area below 21 m (however, the latter occurred mainly in Important polders). Minor reverse transition probabilities can also be detected in the three periods. The elevation of maximum transition probability from Wetland to Urban gradually decreased from 19 m to 17 m over the three time periods.

Low Elevation Land-cover Change by Polder Type 1987 to 2004

Most of the land area in the study area below 21 m, other than Wetland/Water, is protected by the levees and in polders, including almost all (>99 percent) of Farmland below this high-water level. Therefore, a complete analysis of vulnerability needed to consider distribution of these land

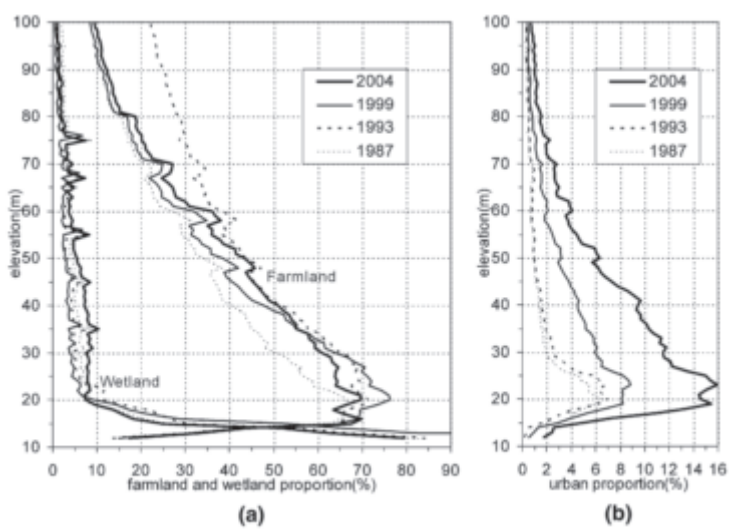

Figure 3. Area proportions of different land-cover types on the landscape by elevation: (a) farmland and wetland proportion percent, and (b) urban proportion percent.

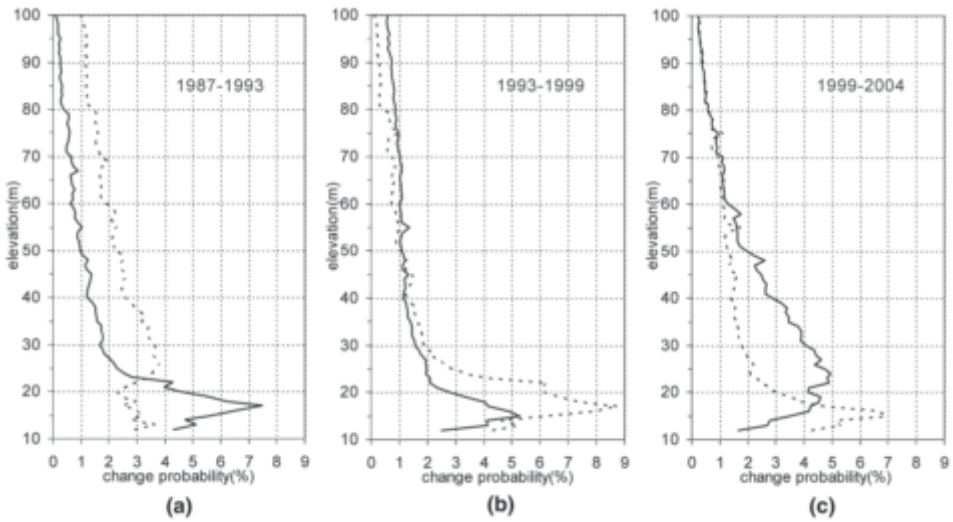

Figure 4. Change probabilities between farmland and wetland area (solid = farmland → wetland, dashed = wetland → farmland): (a) 1987 to 1993, (b) 1993 to 1999, and (c) 1999 to 2004.

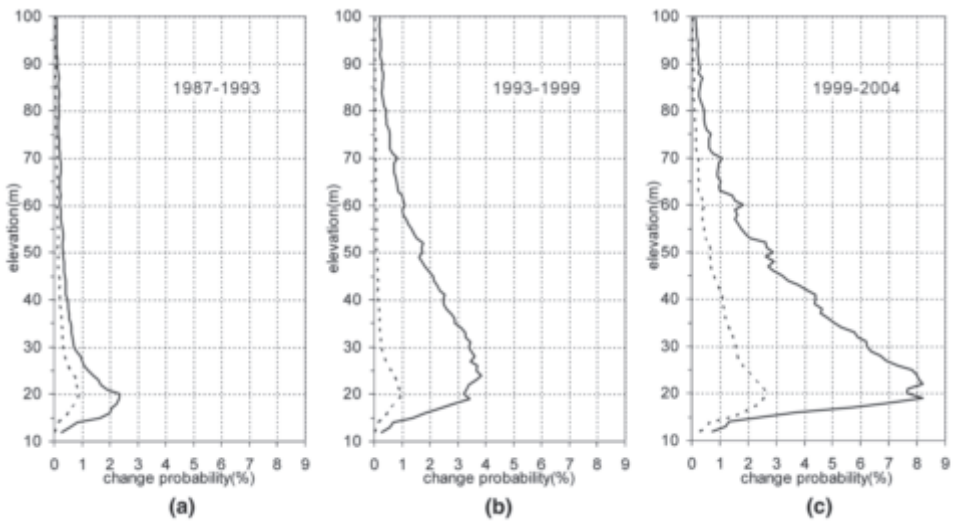

Figure 5. Change probabilities between farmland and urban area (solid = farmland → urban, dashed = urban → farmland): (a) 1987 to 1993, (b) 1993 to 1999, and (c) 1999 to 2004.

covers by polder type. The area of Farmland in Most Important, Important and Storage polders was very stable over the study period. Only in 2004 did the area of Farmland decrease somewhat and mainly because this area transitioned to Urban. In the Small polders, the Farmland area proportion decreased over the later two dates, likely because some of these polders were converted to Partial or Complete Return polders. The areal proportion of Urban increased in the Most Important, Important and Storage polders but decreased in the Small polders. The proportion of Urban area in Most Important polders (~50 percent) was higher than that of Farmland area (<40 percent) in each year (Figure 7).

Discussion

One approach to social vulnerability assessment involves detailed statistical data on the human population, such as that from census data on demographic and economic characteristics (e.g., Cutter *et al.*, 2003). This approach has the advantage of providing detailed information on the characteristics of the population, but provides little information on the spatial distribution of vulnerability to flooding as it is tied to land-use and environmental gradients, such as elevation. Although an eventual model-based approach might provide for a more explicit characterization of flood return intervals, the present analysis based on elevation and levee

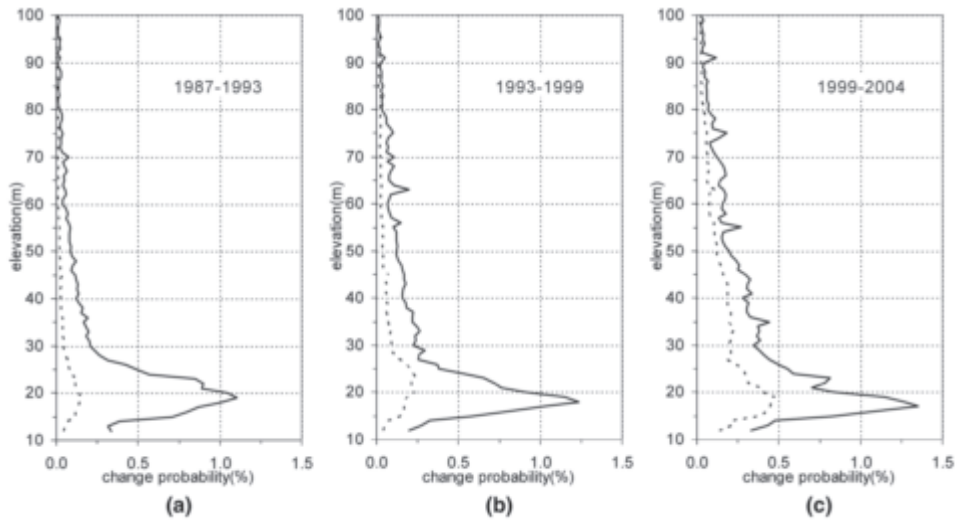

Figure 6. Change probabilities between wetland and urban area (solid = wetland → urban, dashed = urban → wetland): (a) 1987 to 1993, (b) 1993 to 1999, and (c) 1999 to 2004.

maps accounts for the key factors structuring the spatial variability in flood risk. The analysis reveals land-cover changes that are likely the result of policy and economic changes, that are a determinant of vulnerability to flooding, and that may feed-back into future land-use.

Using data on land-cover, levees, the polders they enclose, and elevation we interpreted the effects of the spatial distribution of land covers and land-cover change on flood vulnerability in the PLR. To characterize the exposure to flood risk, we used a DEM and mapped levees and examined the relationships between mapped land-cover and land-cover change, especially for Farmland, Wetland, and Urban, as shown in the previous section. The following interpretation of vulnerability was based on three propositions: (a) lands at lower elevations are at greater risk from flooding; (b) location of human-managed land-cover classes, i.e., Farmland and Urban, in these areas at high risk for flooding are associated with high vulnerability, and flooding of Wetland/Water areas with low vulnerability; and (c) this risk is mediated by the presence of levees forming polders, and the types of polders further structure the patterns of vulnerability and feed-back on future vulnerability.

Spatial Variation in Vulnerability

The highest flood ever recorded on Poyang Lake (20.75 m) and the average annual high-water level (17.3 m) are two key indicators of how elevation is related to flood risk. Overall, our analysis shows that land-cover changes at elevations >21 m accounted for a much greater proportion of all transitions than did changes at elevations <21 m. For example, although some newly urbanized areas were developed below 21 m (Figure 3), development occurred with much greater frequency in areas of low flood risk (>21 m). Similarly, though changes in Farmland exhibited less consistent trends over 17 years, observed increases in farmland tended to occur at elevations >21 m (especially >35 m). This suggests that the patterns of urban development and new farmland are such that increases in the numbers of lives and livelihoods vulnerable to flooding are not as great as they could be.

Still, there were significant areas of Farmland and Urban land covers below 21 m (Figure 3). The levees provide critical protection to the polder areas for the people who farm and reside in this area. The land within the Most Important and Important polders has a relatively low flood risk. None of the levees surrounding these Most Important or Important polders broke even during the tremendous flood of 1998. A relatively stable majority of Farmland (~63 percent) and Urban (70 to 75 percent) land covers below 21 m were in these two polder types throughout the 17-year study period, suggesting a relatively low degree of vulnerability. Many of the levees surrounding Small polders failed in the 1998 and other floods. The creation of the Complete and Partial Return polders changed the level of protection in these Small polders. The Storage, Partial Return, and Complete Return polders are intended to be deliberately filled with water in the largest floods to increase flood storage. The proportion of agriculture in the Storage, Small, and Return polders was constant throughout the 17-year period. Because the Return polders were established to serve as flood storage areas, any remaining farms are now more vulnerable to damage during a large flood.

The proportion of Urban in Small and Return polder types declined, especially in Small polders converted to Return polders which required residents to relocate. These trends suggest declining vulnerability of urban areas to flooding as residents relocated to higher elevations are less vulnerable to flooding. The Urban proportion increased in the Storage polder type. Though the Storage polder type was built to regulate extreme floods, Storage polders have never been used for this purpose, not even in case of the most severe flood of 1998. However, the new Urban areas in the Storage polders may have high vulnerability if the Storage polders are used to regulate severe floods in the future.

The land-cover-change results show that, especially during the latter two time periods (1993 to 1999 and 1999 to 2004), it is in the areas that are most vulnerable to flooding (i.e., low elevation and smaller polders) that Wetland/Water were most likely to have been converted to Farmland, thereby increasing the vulnerability of crops to flooding

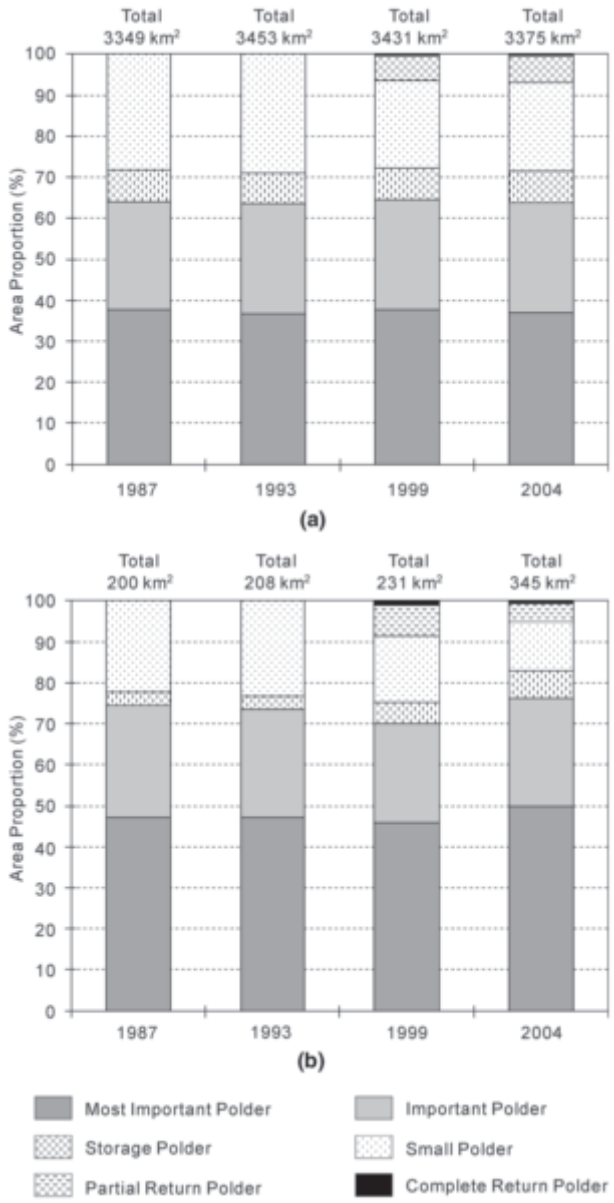

Figure 7. Farmland and urban area change within polders of different types: (a) farmland, and (b) urban.

(Figure 4). Most of the urbanization came at the expense of agriculture, and the peak elevations at which these conversions happened increased from the earliest period to the latter two periods (Figure 5). This suggests a decline in the vulnerability of new urban areas. The peak elevations of urbanizing wetland declined over time (Figure 6), but these new urban areas were significantly less abundant than those occurring in previously agricultural areas.

Relationship of Observed Land-cover Changes in the PLR to Policy

The patterns of land-cover change can reveal not only changes in the relative vulnerability of human populations and their farming systems to flooding, but also provide information about the drivers behind the land-cover change. By relating these drivers to changes in vulnerability, through their effects on land-cover patterns, results may inform policy decisions that might have direct or indirect effects on the vulnerability of the population in the PLR.

The Land Management Law of China, as established in 1986, bans wetland reclamation for farm or urban land-uses. The Law established that the areas of natural rivers, lakes, forests, grasslands and urban centers belong to the national government. The land in rural areas (including the farmlands, ponds and villages), however, are collectively owned by local communities. This dichotomous land-ownership system may have influenced the vertical distribution of land-cover changes in the PLR. According to the elevation analysis of land-cover change in the several years after wetland reclamation was banned (1987 to 1993), probabilities of Wetland conversion to Farmland were reduced below 21 m (Figure 6), where the natural water areas that belong to the national government are mainly located, but remained high at elevations above 21 m. The Wetland/Water in this area is primarily collectively owned by the local community and probably was largely not influenced by the regulation of 1986.

By the period of 1993 to 1999, China had already transitioned into a market economy system. Grain prices increased during this period, and this caused an increase of farming activity. The PLR has been a traditionally important grain production base for China, and as a result land-cover changes from Wetland to Farmland increased during this period (Figure 4). The grain price decreased between the late-1999 and the end of 2003. During this time, farmers were reluctant to plant grain crops in many areas and some areas of Farmland were abandoned. After the flood disaster in 1998, a wetland restoration policy was implemented in the area of this study. These two reasons may have caused the increase of land-cover change from Farmland to Wetland/Water as seen over a wide elevation range (Figures 3 and 4). Consistent with the changes in grain prices, the changes from Wetland to Farmland decreased 1999 to 2004 compared to 1993 to 1999. Small polders are generally protected by earthen levees, which were built with funds from local governments and are not as substantial as the Most Important and Important polders. Dozens of Small polders were planned for wetland restoration (i.e., partially or completely returned to wetland through breaching) in 1998. This may be the main reason for the decline of Farmland area proportion in Small polders between 1993 and 1999, contrary to the increases elsewhere that are consistent with increasing grain prices.

As with elsewhere in China, the PLR has experienced significant amounts of urbanization over the past 20 years. The patterns of transition from Farmland to Urban (Figure 5) are representative of the extensive and accelerating urbanization. Generally, it can be expected that built-up urban area cannot transition into farmland. However, based on the Landsat analysis, this process did occur in the study area. While it is likely that some of these transitions are the result of classification errors, in fact some of these transitions are reasonable in the context of the PLR. The Urban category in this study not only includes the urban area in cities, but also built-up areas for residences, mines, factories, etc. in towns, and villages in rural settings. In 1998, the Land Management Law of China was revised to stress the importance of protecting basic farmland (approximately 80 percent of Chinese farmland is in this category) to ensure the grain security. The Law requested that a county balance and ensure the amount of farmland (called the "occupation and compensation balance" policy). In the PLR, some abandoned built-up areas, mostly in more rural settings, were restored as farmland to meet this requirement for the distribution of basic farmland. Furthermore, when the wetland restoration policy was established in 1998,

there was also a resettlement project in the PLR. With the assistance of subsidies provided by the Chinese government, 905,000 people (220,000 households) whose residences were in the high-risk polders were resettled to lands at elevations above 21 m. Most of their former residence areas were restored to farmland or wetland. Because of the establishment of resettled communities at higher elevations, this latter policy also contributes to the abrupt increase in the probability of change from Farmland to Urban at elevations of above 21 m (Figures 5 and 6).

Conclusions

Large areas of land-cover in PLR have historically been vulnerable to flooding, and levees were built to create polders to cope with this flood risk. In this process, wetlands were reclaimed for farmland and residences. In this paper, different patterns of land-cover and change were described according to their location relative to elevation and, at low elevations, also to polders of several types. Analysis of the distribution of different land covers and changes relative to elevation and polder types provided a useful approach for understanding flood risk and vulnerability. More specifically, the patterns of farmland, wetland, and urban land covers provided important indications of human vulnerability to the flooding.

The land-cover patterns and changes in the PLR over the last 20 years suggest a general decline in vulnerability to flooding, likely driven by policy changes that reduce dependence of the population on grain production and that focus on flood management and flood defense. Most new urban areas and farmland, built to respond to demographic and economic demand, were occurring at elevations higher than the highest recorded flood, or in polders that are protected by the levees that are least likely to fail, especially later in the period. The relative proportion of urban areas in the smallest, most vulnerable polder areas declined significantly, as new urban development occurred more frequently in the larger polders and as some communities were resettled to higher elevations. The breaching of levees for the purposes of increasing flood-storage capacity of the lake places some farmland areas at greater risk from flooding, but the policies are well known and the damages can be mitigated through education of residents.

Understanding vulnerability in the context of adaptable human societies requires placing the spatial and temporal variability of flood hazards within the context of options and processes of human response at multiple levels (e.g., individuals and governments). The payoff from studies applied to land-use and flooding is in the new understanding of how the interactions of human behavior and environmental variability yield both vulnerability and resilience in these coupled systems. The analysis reported in this paper sets the stage for more dynamic model-based analyses of such vulnerability in the PLR, but is focused on understanding geographic patterns and temporal human-driven changes of land-cover relative to locations that are at risk from flooding.

Acknowledgments

We acknowledge financial support for this project from the U.S. National Aeronautics and Space Administration (NASA Grant No. NEWS/04–1–0000–0025), the U.S. National Science Foundation (NSF Grant No. BCS-0527318), the National Science Foundation of China (NSFC Grant No. 40561011), and the Key Laboratory of Poyang Lake Ecological Environment and Resource Development (Jiangxi Normal University). We also wish to thank Shuming Bao, Lin Zheng, and Ying Liu for their collaboration and support on arranging for logistics in the field.

References

Chander, G., and B. Markham, 2003. Revised Landsat-5 TM radiometric calibration procedures and postcalibration dynamic ranges, *IEEE Transactions on Geoscience and Remote Sensing*, 41(11):2674–2677.

China Meteorological Administration, 2007. China Meteorological Data Sharing Service System, URL: http://data.cma.gov.cn (last date accessed: 13 February 2008).

Congalton, R.G., and K. Green, 1999. *Assessing the Accuracy of Remotely Sensed Data: Principles and Practices*, Lewis Publishers, Boca Raton, Florida.

Cutter, S.L., B.J. Boruff, and W.L. Shirley, 2003. Social vulnerability to environmental hazards, *Social Science Quarterly*, 84(1):242–261.

Data Center for Resources and Environmental Sciences, Chinese Academy of Sciences, 2003. 1:100 000 Land-use/Cover Database of China, URL: http://www.resdc.cn (last date accessed: 13 February 2008).

Definiens, 2006. *Definiens Professional 5 User Guide*, Version 5.0.6.1, Definiens AG, München, Germany.

Editorial Committee of Poyang Lake Research, 1988. *Poyang Lake Research*, Shanghai Publishing House on Science and Technology, Shanghai, China.

ESRI, 2007. ArcGIS®9.2. Environmental Systems Research Institute, Redlands, California.

Gale F., B. Lohmar, and F. Tuan, 2005. China's New Farm Subsidies, USDA/ERS, URL: http://ers.usda.gov/publications/WRS0501 (last date accessed: 13 February 2008).

Irish, R., 1998. Landsat 7 Science Data Users Handbook: Chapter 11, Data Products. URL: http://ltpwww.gsfc.nasa.gov/IAS/handbook/handbook_toc.html (last date accessed: 13 February 2008).

Jiang, L.G., 2006. *Flood Risk and Land-use Change in the Wetland Restoration Area Around Poyang Lake, China*, Ph.D. dissertation, Institute of Geographic Sciences and Natural Resources Research, Chinese Academy of Sciences, Beijing, China.

Jiangxi Province Department of Water Resources, 1999. *Levee Atlas of Jiangxi Province*, Nanchang, China.

Leica Geosystems, 2005. *ERDAS Imagine® 9.0*, Leica Geosystems, Heerburg, Switzerland.

Liverman, D., E.F. Moran, R.R. Rindfuss, and P.C. Stern, (editors), 1998. *People and Pixels: Linking Remote Sensing and Social Science*, National Academy Press, Washington, D.C.

Li, R.D., and J.Y. Liu, 2001. An estimation of wetland vegetation biomass in the Poyang Lake using Landsat ETM data, *Acta Geographica Sinica*, 56(5):532–540.

Liu, X., M. Chen, W. Chen, L. Huang, and Z.H. Xiao, 2005. Variation of cultivated land and its driving forces in Poyang Lake area, *Journal of Jiangxi Agricultural University*, 27(2):309–312.

Min, Q., 2004. On the restoring lake by stopping cultivation to Poyang Lake and its impacts on flood mitigation, *Journal of Lake Sciences*, 16(3):215–222.

Ojima, D., and E. Moran (IGBP/IHDP Transition Team Members), 2004. Global Land Project Science Plan, URL: http://www.globallandproject.org (last date accessed: 13 February 2008).

Rao, S., J.Y. Fang, H.T. Cui, and G.C. Lei, 2002. Spatio-temporal changes in patterns of land-use in Poyang Lake during the last decade, *Resources and Environment in the Yangtze Basin*, 11(5):421–426.

Rozelle, S., G. Veeck, and J.K. Huang, 1997. The impact of environmental degradation on grain production in China, 1975–1990, *Economic Geography*, 73(1):44–66.

Shankman, D, and Q. Liang, 2003. Landscape changes and increasing flood frequency in China's Poyang Lake Region, *Professional Geographer*, 55(4):434–45.

Shibayama, M, and T. Akiyama, 1989 Seasonal visible, near-infrared and mid-infrared spectra of rice canopies in relation to LAI and above-ground dry phytomass, *Remote Sensing of Environment*, 27(2):119–127.

State Bureau of Surveying and Mapping of China, 1972. 1:50000 Topographic Map of China, URL: http://data.sbsm.gov.cn/mapquery/index.aspx (last date accessed: 13 February 2008).

State Forestry Administration of China, 2003. *China National Wetland Conservation Action Plan*, China Forestry Publishing House, Beijing, China.

Statistics Bureau of Jiangxi Province, 2004. *Statistical Yearbook of Jiangxi Province*, China Statistic Press, Beijing, China.

Tou, J.T., and R.C. Gonzalez, 1974. *Pattern Recognition Principles*, Addison-Wesley Publishing Co., Reading, Massachusetts.

Tucker, C.J., D.M. Grant, and J.D. Dykstra, 2004. NASA's Global orthorectified Landsat data set, *Photogrammetric Engineering & Remote Sensing*, 70 (3):313–322.

Wang, Q., M. Watanabe, S. Hayashi, and S. Murakami, 2003. Using NOAA AVHRR data to assess flood damage in China, *Environmental Monitoring and Assessment*, 82:119–48.

White, G.F., and J.E. Haas, 1975. *Assessment of Research on Natural Hazards*, MIT Press, Cambridge, Massachusetts.

Xiao, X., S. Boles, S. Frolking, W. Salas, B. Moore, C. Li, L. He, and R. Zhao, 2002. Observation of flooding and rice transplanting of paddy rice fields at the site to landscape scales in China using VEGETATION sensor data, *International Journal of Remote Sensing*, 23:3009–3022.

Yin, H.F., and C.A. Li, 2001. Human impact on floods and flood disasters on the Yangtze River, *Geomorphology*, 41:105–109.

Zhao, S., J. Fang, W. Ji, and Z. Tang, 2003. Lake restoration from impoldering: Impact of land conversion on riparian landscape in Honghu Lake area, Central Yangtze, *Agriculture Ecosystems and Environment*, 95(1):111–118.